TESLA - COLLABORATION

FIELD MEASUREMENT SIMULATION AND MEASUREMENT ERROR ESTIMATION IN TESLA CAVITIES AT ROOM TEMPERATURE

M.Dohlus, N.Holtkamp
Deutsches Elektronen-Synchrotron DESY
Notkestr.85, 22607 Hamburg, Germany

V.Kaljuzhny
Moscow State Engineering Physics Institute MEPhI
(Technical University)
Kashirskoe sh. 31, 115409, Moscow, Russia

November 1998, TESLA 98-27

FIELD MEASUREMENT SIMULATION AND MEASUREMENT ERROR ESTIMATION IN TESLA CAVITIES AT ROOM TEMPERATURE

M.Dohlus, N.Holtkamp
Deutsches Elektronen-Synchrotron DESY
Notkestr.85, 22607 Hamburg, Germany

V.Kaljuzhny
Moscow State Engineering Physics Institute
(Technical University)
Kashirskoe sh. 31, 115409, Moscow, Russia

Abstract

The field measurement accuracy in niobium TESLA cavities at room temperature is estimated. The requirements for a perturbing body and measured quantities (reflection coefficients S_{11} or S_{22}, transmission coefficients $S_{21}=S_{12}$, $\varphi_{21}=\arg S_{21}$ and $d\varphi_{21}/df$) were established. It was shown that field measurement error could achieve 20% in the 4×7=28-cell cavities with an operational 0-π-mode and low quality factor of the cells ($Q_0=10^4$). A measurement error achieves 7% in the 4×7=28-cell cavity with a quality factor of the cells $Q_0>2.5\times10^4$ (a copper cavity) and 3% in the 4×7=28-cell superconducting TESLA cavity.

I. Introduction

The TESLA superconducting cavities must be preliminary tuned at room temperature. Tuning accuracy is defined by an experimentally measured field distribution along the cavity. We shall study a field measurement error in the cavities of two types: in 9-cell TESLA cavity with an operational π-mode and in 4×7=28-cell TESLA supercavity with an operational 0-π-mode [1]. Parameters of these cavities are shown in Table 1.

Table 1

	Usual cavity	Supercavity
$E_{acc\ eff}$, MV/m	25	25
f_{op}, GHz	1.3	1.3
K_{loss}/N_{cells} , V/C	2.35×10^{11}	2.13×10^{11}
τ_{op} , sec	746.1×10^{-6}	823.1×10^{-6}
Q_{ext}	3.0472×10^{6}	3.3616×10^{6}
τ_{op}/T_{RF}	0.560982	0.618877
t_{b1}, sec	517.162×10^{-6}	570.534×10^{-6}

Where $E_{acc\ eff}$ is an effective accelerating field strength,
f_{op} is an operational frequency,
K_{loss}/N_{cells} is a loss parameter per cell,
τ_{op} is an operational mode decay time,
Q_{ext} is an external Q-factor of the cavity,
T_{RF} is RF pulse duration,
t_{b1} is a time moment of the first bunch passage through the cavity.

These parameters correspond to the following beam parameters:
bunch repetition frequency $f_b=f_{op}/920=1.413043478$ MHz,
number of the particles in the bunch $N_{be}=3.63\times10^{10}$
(bunch charge $q_b=5.81594$ nC, pulse beam current $I_b=8.218186$ mA).

At the room temperature Q_0-factor of the niobium TESLA cavity is equal to 10^4 and $Q_{ext}\approx(3.0\text{-}3.3)\times10^6$. It means that coupling coefficient between the cavity and an input waveguide $\chi\approx3\times10^{-3}$ and an input reflection coefficient is very close to 1. The neighbouring mode frequency is close to the operational mode frequency. All these peculiarity of the niobium TESLA cavity at room temperature can cause a large field measurement error.

We shall base our arguments on the fundamental work [2] on the theory of field strength determination in RF structures by perturbation techniques and simulate field measurement using equivalent circuit of the investigated cavity [3]. We shall consider a two-port junction consisting of the investigated cavity and two waveguides coupled with the cavity cells (input and output waveguides can be coupled with different or the same cell).

A perturbation technique consists of the introduction of a small perturbing body (in our case needle) into the some part of the investigated structure and the measurement of the resultant change in some characteristics of the structure observable in an output lead (e.g. a resonant frequency of the operational mode, input reflection

coefficient, transmission coefficient, phase of transmission coefficient and so on).

There are some fundamental perturbation formulae derived in the work [2] [(19), (20), (24), (25)]

$$\frac{\Delta f_{cav}}{f_{cav}} = -\frac{\sum_{i=x,y,z}\{k_i^{(E)}|E_i|^2 + k_i^{(B)}|B_i|^2\}}{4W_{cav}}, \quad \Delta\left(\frac{1}{Q_{cav}}\right) = \frac{\sum_{i=x,y,z}\gamma_i|E_i|^2}{2\omega_{cav}W_{cav}} \qquad (1)$$

$$\Delta S_{k,m} = -\frac{j\omega}{4\sqrt{P_k P_m}}\sum_{i=x,y,z}\{k_i^{(E)}E_i^{(k)}E_i^{(m)} - k_i^{(B)}B_i^{(k)}B_i^{(m)} + \frac{1}{j\omega}\gamma_i E_i^{(k)}E_i^{(m)}\} \qquad (2)$$

The expression (1) are perturbation formulae for a resonant perturbation technique. Here

$\Delta f_{cav}/f_{cav}$ is the relative shift in the free oscillation frequency of the operational mode,

$\Delta f_{cav}=f^{(p.b.)}-f_{cav}$,

$f^{(p.b.)}$, f_{cav} are the free oscillation frequencies in an operational mode with and without a small perturbing body in the cavity respectively,

$\omega_{cav}=2\pi f_{cav}$,

$k_i^{(E,B)}$, γ_i are the form factors of a small perturbing body,

E_i , B_i are the components of the unperturbed free oscillation field vectors at the position of the perturbing body,

W_{cav} is the total energy stored in the cavity.

These formulae were derived under the assumption that perturbed and unperturbed fields are approximately equal to each other and the cavity is essentially lossless. These formulae show that $E\propto(\Delta f_{cav}/f_{cav})^{1/2}$ in our measurements (a needle moves along the cavity axis). But, as it will be shown, this assumption may be broken for the 4×7-cell niobium TESLA cavity at room temperature. Perturbed and unperturbed fields may be very different from each other and a resonant perturbation technique formulae (1) may give a large error. Some difficulties occur in the measurement of the free oscillation frequency in the perturbed and unperturbed cavity.

In general a perturbation technique formula has the following view (see work [2], formula (16))

$$\frac{\omega^{(p.o.)}-\omega_{cav}}{\omega_{cav}}=\frac{\sum_{i=x,y,z}\left(k_i^{(E)}E_i^{(p.o.)}E_i-k_i^{(B)}B_i^{(p.o.)}B_i\right)+\frac{1}{j\omega_{cav}}\sum_{i=x,y,z}\gamma_i E_i^{(p.o.)}E_i}{\int_V\left(\varepsilon\vec{E}^{(p.o.)}\vec{E}-\mu\vec{H}^{(p.o.)}\vec{H}\right)dv} \qquad (3)$$

Here $\omega^{(p.o.)}$ and ω_{cav} are the angular frequencies of the free oscillation in an operational mode with and without a small perturbing body in the cavity respectively,

$\vec{E}^{(p.o.)}$, $\vec{H}^{(p.o.)}$ and $\vec{E}$, $\vec{H}$ represent a field vectors of the perturbed and unperturbed free oscillation,

$\mathbf{E}_i^{(p.o.)}$, $\mathbf{B}_i^{(p.o.)}$, $\mathbf{E}_i$, $\mathbf{B}_i$ are the components of the corresponding perturbed and unperturbed field vectors at the position of the perturbing body.

If there is any lossy material in the external medium or the perturbing body, $\omega^{(p.o.)}$ and ω_{cav} will become complex quantities of course.

The expression (3) contains the product of the unperturbed and perturbed field vectors at the position of the perturbing body. This expression is very complicated for a field measurement application.

The expression (2) is a perturbation formula for a nonresonant perturbation technique. Here

$\Delta S_{k,m}=\Delta S_{m,k}=S_{k,m}^{(p.b.)}-S_{k,m}$ is the change in the transmission coefficient from the k-th port in the m-th port (k, m =1,2 in our case),

$S_{k,m}^{(p.b.)}$, $S_{k,m}$ are the transmission coefficients with and without a small perturbing body in the cavity,

ω is an angular frequency, at which measurement is carried out,

$E_i^{(k)}$, $B_i^{(k)}$ are the components of the field vectors of the unperturbed field set up by the input power P_k (incident wave power) in the k-th port (the m-th port is terminated by a matched load),

$E_i^{(m)}$,$B_i^{(m)}$ are the components of the field vectors of the unperturbed field set up by the input power P_m (incident wave power) in the m-th port (the k-th port is terminated by a matched load).

If k=m then we have $E_i^{(k)}E_i^{(m)}=(E_i^{(k)})^2$, $B_i^{(k)}B_i^{(m)}=(B_i^{(k)})^2$ and ΔS_{kk} is the change in the reflection coefficient in some reference plane of the k-th port. $E_i^{(k)}$, $E_i^{(m)}$, $B_i^{(k)}$, $B_i^{(m)}$, $\Delta S_{k,m}$ are the complex quantities of course.

Formula (2) for k=m shows that a nonresonant perturbation technique gives us an information about an absolute value and phase of the unperturbed forced oscillation field at a given frequency $\omega=2\pi f$ and under a given cavity excitation condition. In our case field distribution of the forced and free oscillation may be very different from each other and, moreover, reflection coefficient is very close to unit.

To simulate a field measurement and estimate a measurement error we use an equivalent circuit of the investigated cavity shown in Fig.1.

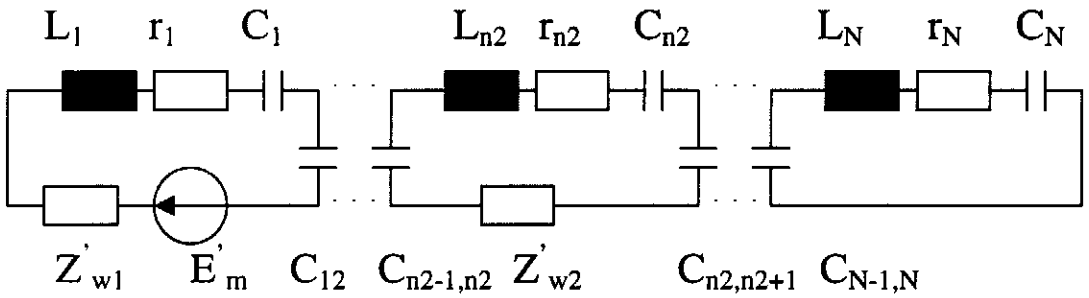

Fig.1. Equivalent circuit for a field measurement simulation.

Here Z'_{w1} and Z'_{w2} are the wave impedances of the input and output waveguides inserted into the loops of the n1-th (n1=1 in the figure) and n2-th cell, E'_m is a generator e.m.f. inserted into the loop of the n1-th cell. N is a number of cells in the cavity.

The equivalent circuit permits us to calculate a complex scattering matrix coefficients $S_{1,1}$, $S_{2,1}=S_{1,2}$, $S_{2,2}$ at a given frequency f and cells detuning. The complex scattering matrix corresponds to some reference planes in the input and output waveguides and a field distribution corresponding to a forced oscillation at a given frequency f. At the same time we can calculate a frequency and a field distribution along the cavity corresponding to a free oscillation. The perturbing body effect can be simulated as a given relative detuning ($\delta f_{nb}/f_n$) of the n-th cell, n=1, 2, 3, ... N and a given relative deterioration ($\Delta Q_{0nb}/Q_{0n}$) in the Q_{0n}-factor of this cell, where f_n and Q_{0n} are a frequency and Q_0-factor of the n-th cell. Thus we can simulate a resonant and nonresonant perturbation technique.

We shall study ability and errors of a resonant perturbation technique. According to the formula (1) we shall find electric field strength as $E\propto(\Delta f_{cav}/f_{cav})^{1/2}$ and compare it with a free oscillation field distribution.

II. FIELD MEASUREMENT SIMULATION IN THE 9-CELL TESLA CAVITY AT ROOM TEMPERATURE

First of all we shall study a field measurement error in the 9-cell TESLA cavity at room temperature. In our simulation we use Q_0-factor of the cells $Q_{0n}=10^4$ (niobium cavity at room temperature), a coupling coefficient between the cells $K_{cn}=1.88988\times10^{-2}$. We assume that input and output waveguides are coupled with the first and the last cell of the cavity (n1=1 and n2=9) and coupling coefficients between the first cell and input waveguide and between the last cell and output waveguide $\chi_1=\chi_9=1.4768\times10^{-2}$ (to provide $Q_{ext}=3.0472\times10^6$, see Table 1).

Let us consider a perfectly tuned cavity. Fig.2 and Fig.3 show a relative field and phase distribution for the free and forced oscillation in the 9-cells cavity.

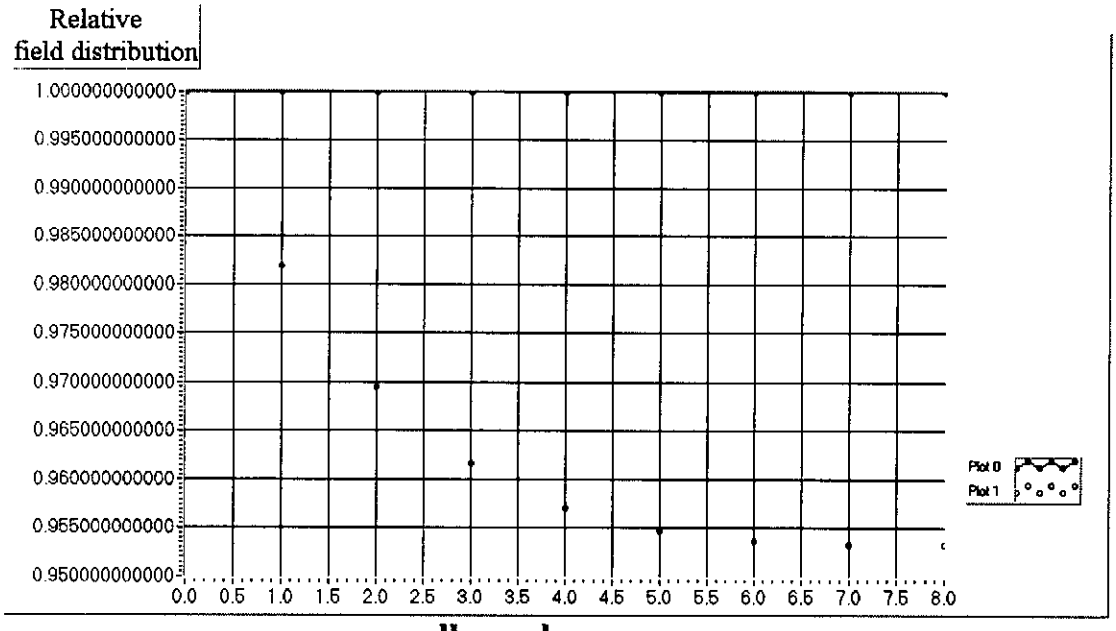

Plot 0 corresponds to free oscillation field distribution along the cavity,
Plot 1 corresponds to forced oscillation field distribution along the cavity.

Fig.2 Relative field amplitude distribution of the free and forced oscillation in the 9-cell niobium TESLA cavity at room temperature.

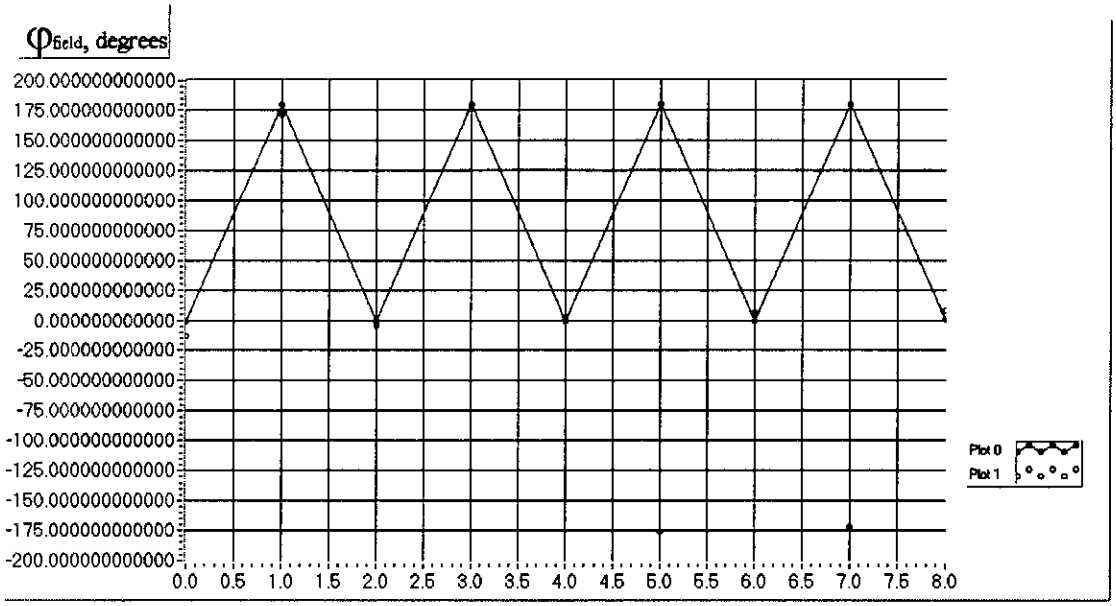

cell number, n

Plot 0 corresponds to free oscillation field distribution along the cavity,

Plot 1 corresponds to forced oscillation field distribution along the cavity,

Fig.3 Phase distribution of the free and forced oscillation in the 9-cell niobium TESLA cavity at room temperature.

One can see that field amplitude distribution of the free and forced oscillation is very close to each other.

We shall simulate a perturbing body effect as relative cells detuning ($\delta f_{nb}/f_n$) caused by a perturbing body and neglect deterioration in the quality factor of the cell.

Usually one of the following frequencies is accepted as a free oscillation frequency:

frequency $f(|S_{11}|_{min})$ at which an absolute value of S_{11} has a minimum,

frequency $f(|S_{21}|_{max})$ at which an absolute value of S_{21} has a maximum,

frequency $f(|d\varphi_{21}/df|_{max})$ at which a slope of the $\varphi_{21}(f)$ dependence has a maximum (where $\varphi_{21}=\arg S_{21}$).

We have an ability to simulate a resonant perturbation technique with all these quantities to find a free oscillation frequency with and without a perturbing body in the cavity. At the same time we can use

an ideal resonant perturbation technique (RPT) using a direct calculation of a free oscillation frequency with and without a perturbing body in the cavity.

We shall study an accuracy of the RPT and it's dependence on a relative detuning of each cell caused by the perturbing body. Let us suppose that a perturbing body causes the same relative detuning in each cell ($\delta f_{nb}/f_n$ does not depend on cell number n) and all cells are perfectly tuned. We know that field amplitude must be the same in each cell in the perfectly tuned cavity at an operational mode frequency. Calculation of free oscillation field distribution confirms it for a superconducting cavity and for a cavity with low Q_0-factor of the cells ($Q_{0n}=10^4$).

Simulation results for a different cell detuning caused by the perturbing body are presented in Table 2. These results were obtained with a direct calculation of a free oscillation frequency without and with the perturbing body in the cavity (with an ideal RPT)).

Table 2

Rel. cell detuning ($\delta f_{nb}/f_n$)	Measurement error, %	Cavity detuning Hz	Remarks
10^{-7}	0.47	15	nonrealistic case
10^{-6}	0.48	143	nonrealistic case
10^{-5}	0.65	1426	acceptable value
5×10^{-5}	1.4	6982-7180	acceptable value
10^{-4}	2.25	13609-14214	acceptable value
10^{-3}	15	89938-124427	very large field perturbation
5×10^{-3}	34	167238-385175	very large field perturbation

One can see that an acceptable relative cell detuning caused by a perturbing body $\delta f_{nb}/f_n=10^{-5}$-$10^{-4}$. We shall use $\delta f_{nb}/f_n=5\times10^{-5}$ in our simulation.

For a perfectly tuned cavity we have obtained the following data:
frequency corresponding to $|S_{11}|_{min}$ is equal to 1299999898 Hz (-100 Hz),
frequency corresponding to $|S_{21}|_{max}$ is equal to 1299990548 Hz (-9450 Hz),
frequency corresponding to $|d\varphi_{21}/df|_{max}$ is equal to 1299999958 Hz (-40 Hz),
free oscillation frequency is equal to 1299999998 Hz.

One can see that frequency $f(|d\varphi_{21}/df|_{max})$=1299999958 Hz is very close to the free oscillation frequency f_{free}=1299999998 Hz (-40 Hz). We shall call a field measurement simulation with these quantities as $f(|S_{11}|_{min})$-, $f(|S_{21}|_{max})$-, $f(|d\varphi_{21}/df|_{max})$-field measurement simulation.

Fig.4 shows a field measurement simulation with different measured quantities and with an ideal RPT.

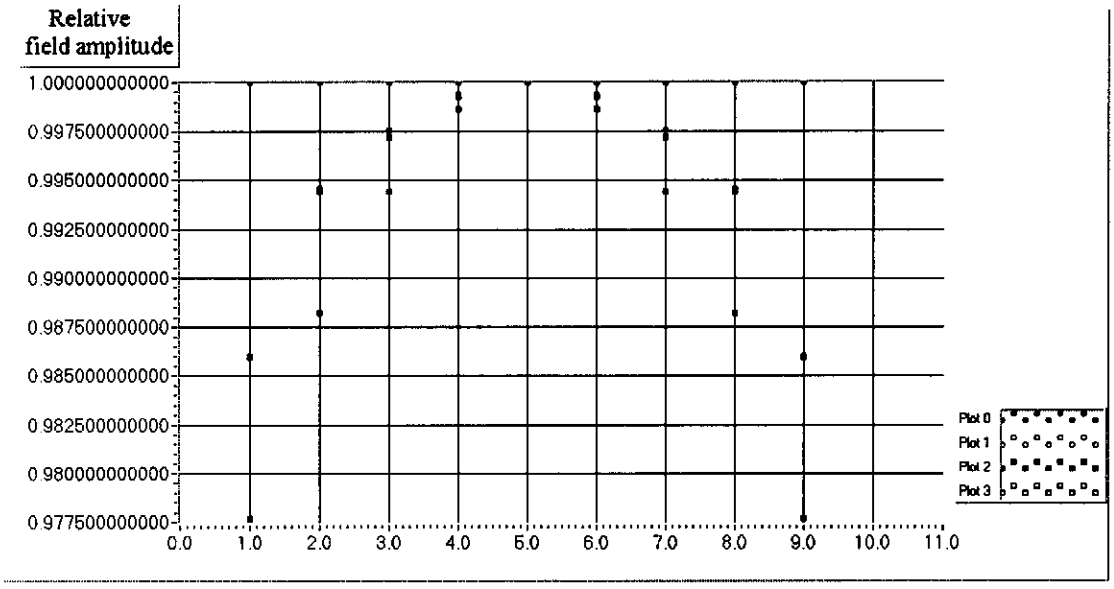

Plot 0 corresponds to a free oscillation field distribution,
Plot 1 corresponds to an ideal RPT,
Plot 2 corresponds to $f(|d\varphi_{21}/df|_{max})$-measurement simulation,
Plot 3 corresponds to $f(|S_{21}|_{max})$-measurement simulation.

Fig.4. Field measurement simulation in 9-cell niobium TESLA cavity at room temperature ($\delta f_{nb}/f_n=5\times10^{-5}$)

One can see that field measurement errors are different for different cells. It can be explained by a different field perturbation when the perturbing body is inserted into different cells. The errors are not large (1.3% --- 2.25%) and we can use any quantity for a field measurement. $f(|d\varphi_{21}/df|_{max})$-measurement simulation and an ideal RPT simulation give very close results.

Fig.5 shows a dependence of φ_{21} on cell number calculated at the free oscillation frequencies when the perturbing body is inserted into different cells.

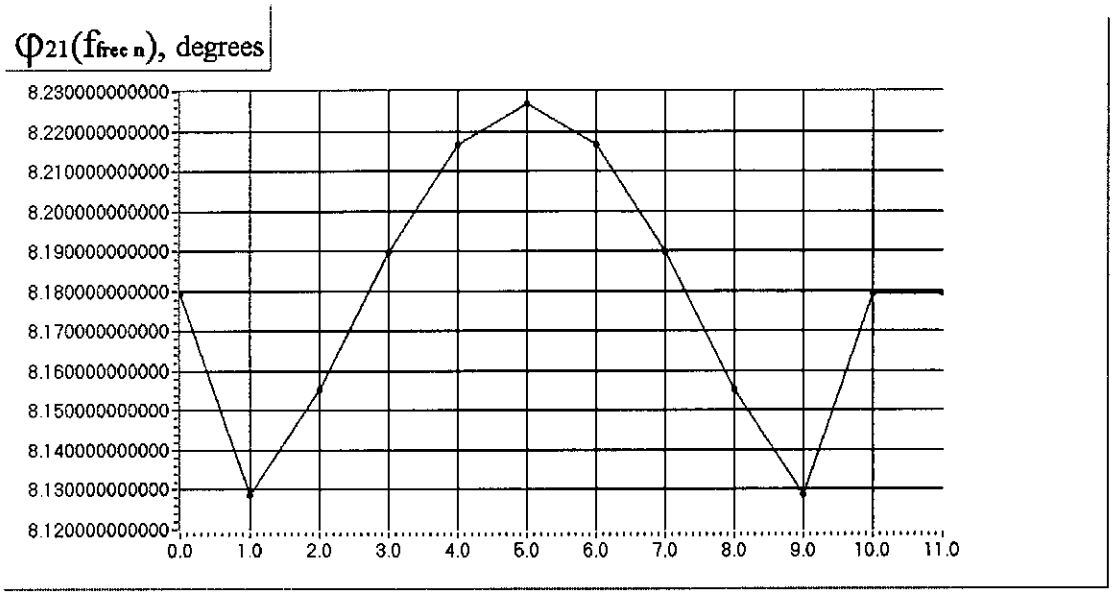

Fig.5. φ_{21} dependence on cell number at $f_{free\ n}$ (n=0,10 and 11 correspond to the cavity without the perturbing body, n=1,2,...,9 correspond to cells number)

One can see very weak dependence of this quantity on cell number. This fact can be used for a field measurement and we shall call such field measurement as φ_{21}-field measurement. Fig.6 shows field measurement simulation result obtained with φ_{21}-field measurement simulation. In this case $E \propto ([f_{free\ n} - f_{free\ 0}]/ f_{free\ 0})^{1/2}$, where $f_{free\ n}$ is a frequency of the free oscillation when a perturbing body is inserted into the n-th cell measured as a perturbed forced oscillation frequency at which $\varphi_{21}=\varphi_{21}(f_{free0})$, f_{free0} is a frequency of the free oscillation without a perturbing body in the cavity. One can see that field measurement error is less then 0.65%. This is the best way for field measurement in the 9-cell TESLA cavity. But this way is not a common way. As it will be shown later this way doesn't give so good result for the 4×7=28-cell TESLA supercavity with an operational 0-π-mode and may give large errors in other cases.

Fig.7 shows an example of φ_{21}-field measurement simulation in the 9-cell cavity in the presence of a random cells detuning having a uniform distribution in the frequency band of ±100 kHz. One can see that measurement error is not large.

In all considered cases an operational π-mode frequency and a neighbouring mode frequency are not very close to each other and we have an ability to find a perturbed and unperturbed free oscillation frequency accurate enough. Fig.8 and 9 shows $|S_{21}|$ and $|S_{11}|$ dependence on frequency for a perfectly tuned 9-cell niobium TESLA cavity at room temperature.

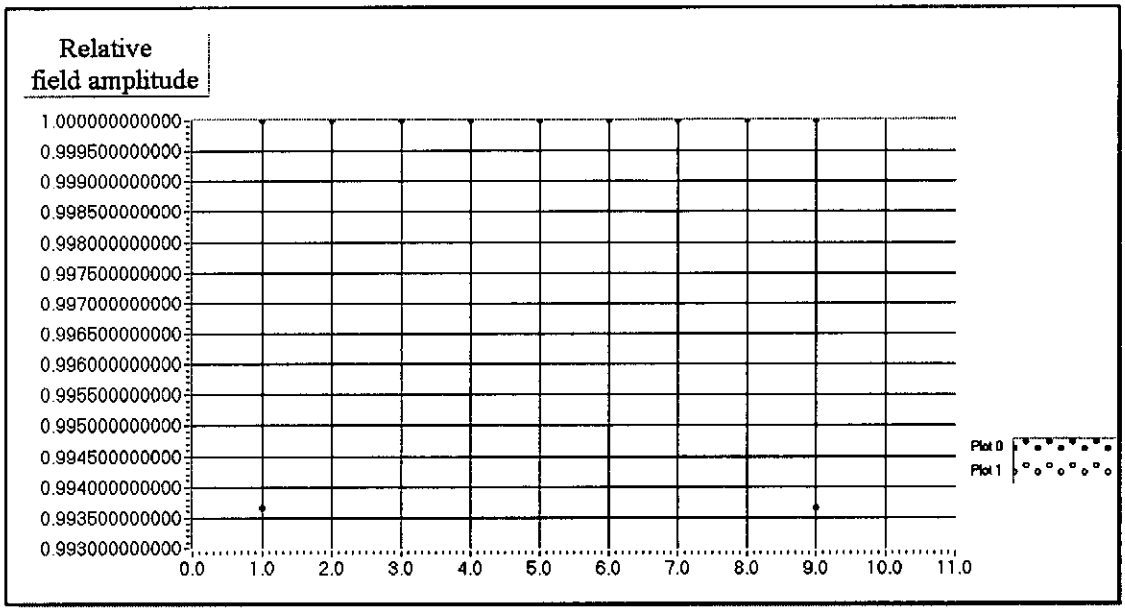

Plot 0 corresponds to free oscillation field distribution,
Plot 1 corresponds to φ_{21}-field measurement simulation.

Fig.6. φ_{21}-field measurement simulation in the 9-cell niobium TESLA cavity at room temperature.

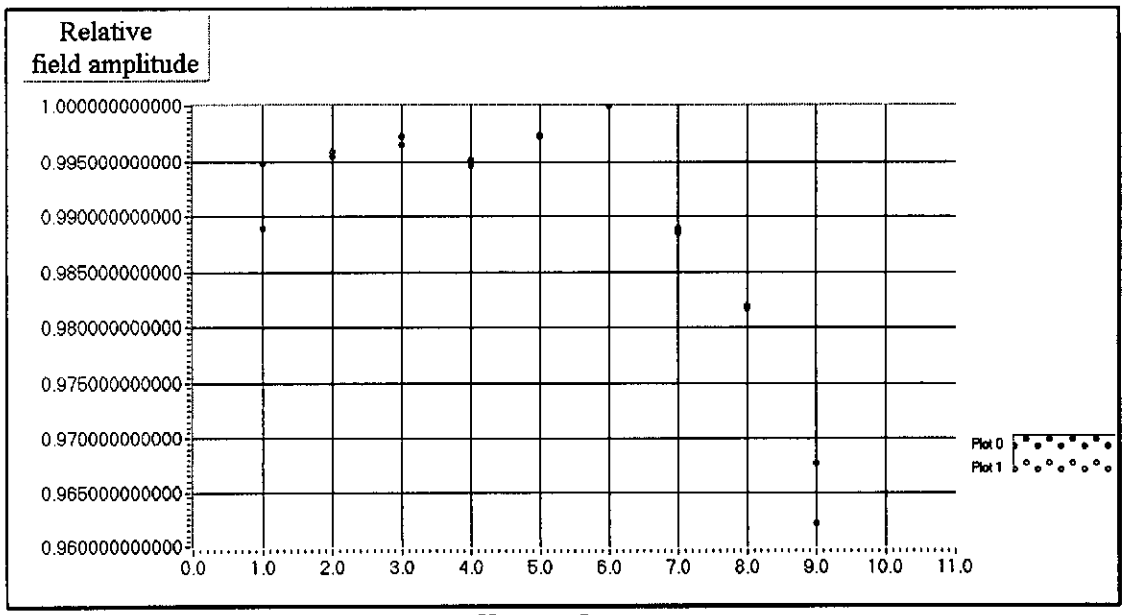

Plot 0 corresponds to free oscillation field distribution,
Plot 1 corresponds to φ_{21}-field measurement simulation.

Fig.7. φ_{21}-field measurement simulation in the presence of random cells detuning ($|\delta f_{cn}| < 100$ kHz)

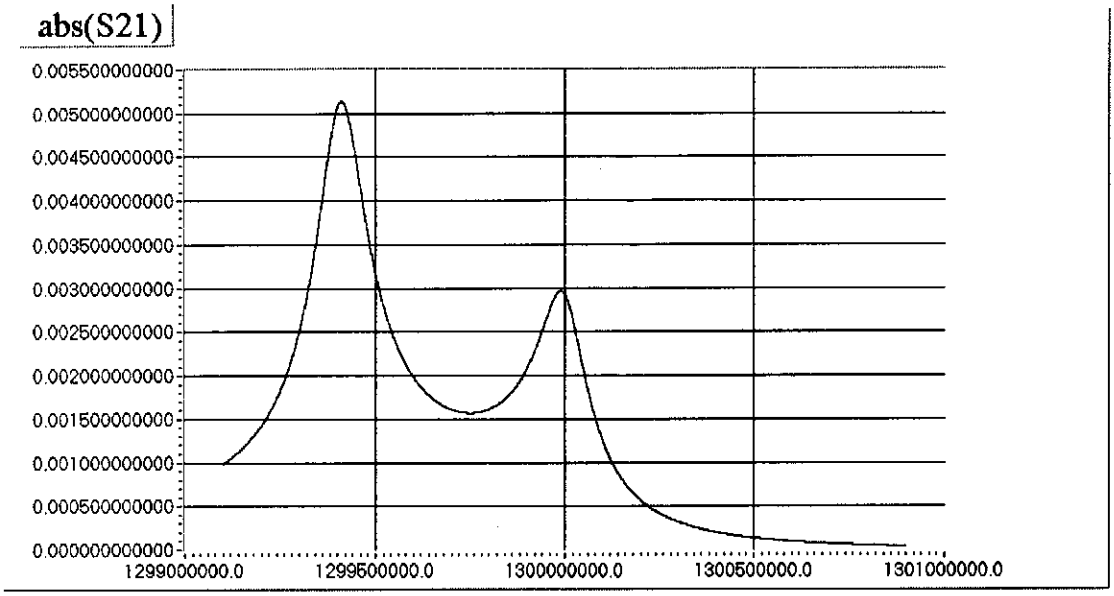

frequency, Hz

(step=100 Hz, span=1.8 MHz)

Fig.8. $|S_{21}|$ dependence on frequency for the perfectly tuned niobium 9-cell TESLA cavity at room temperature.

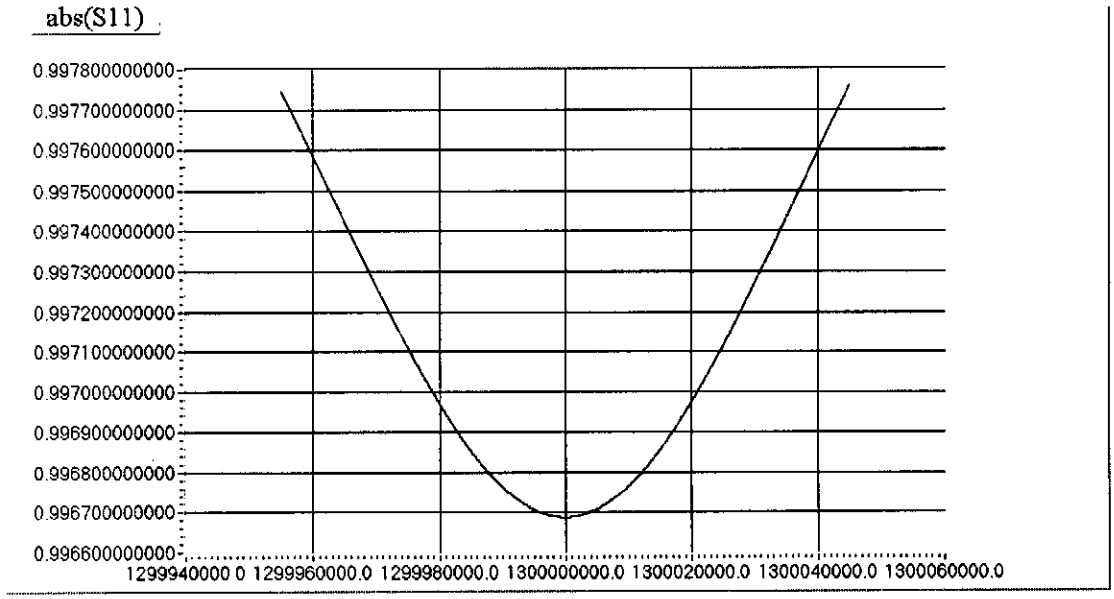

frequency, Hz

(step=10 Hz, span=90 kHz)

Fig.9. $|S_{11}|$ dependence on frequency for the perfectly tuned niobium 9-cell TESLA cavity at room temperature.

III. FIELD MEASUREMENT SIMULATION IN THE 4×7=28- CELLS SUPERCAVITY AT ROOM TEMPERATURE

The 4×7=28-cell supercavity [1] consists of 4 subcavities coupled by a λ/2-length bunch pipes (λ=230.61 mm), which provide 0.002017 coupling coefficient between the cells of the neighbouring subcavities. Cell to cell coupling coefficient in the subcavity is equal to 0.018898.

Let us assume that Q_0-factor of each cell is equal to 10^4 (niobium cavity at room temperature), an input and an output wavequides are coupled with the first and the last cells respectively (n1=1, n2=28). We shall use the coupling coefficient between an input waveguide and the first cell and between an output waveguide and the 28-th cells $\chi_1=\chi_{28}=4.1647\times10^{-2}$ (to provide $Q_{ext}=3.3616\times10^6$, see Table 1) in our simulation.

First of all let us consider a perfectly tuned cavity. Relative field amplitude and phase distribution of the free and forced oscillation in the 4×7=28-cell niobium TESLA supercavity at room temperature are shown in Fig.10 and 11.

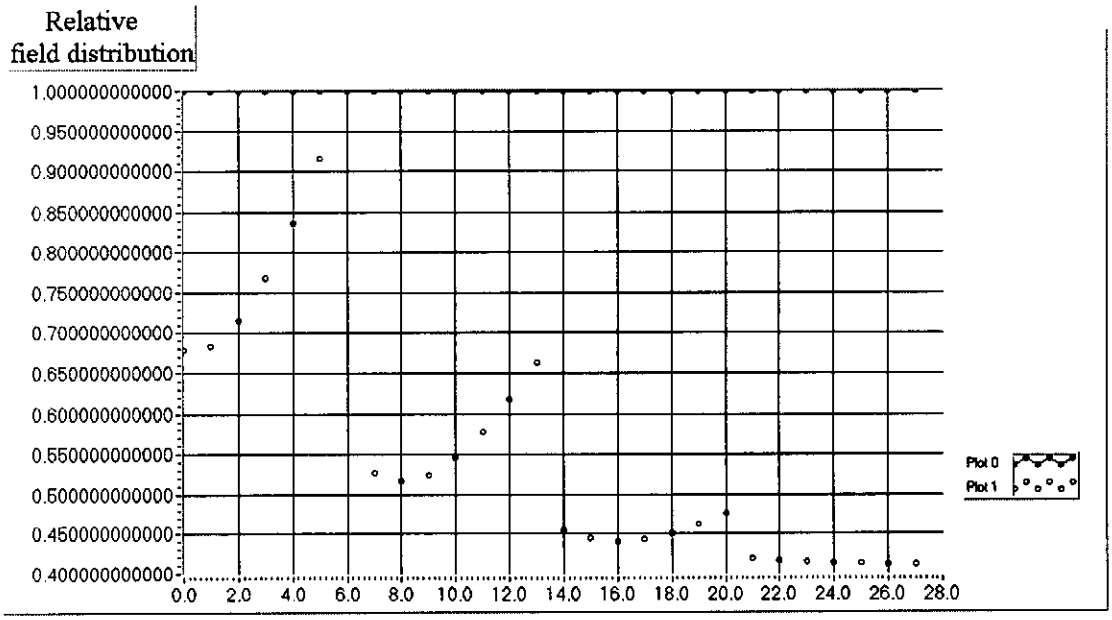

cell number, n

Plot 0 corresponds to free oscillation,

Plot 1 corresponds to forced oscillation at the frequency $f_{op\ free}$=1.299999998241 Hz.

Fig.10.Relative amplitude distribution of the free and forced oscillation in the 4×7=28-cell niobium TESLA supercavity at room temperature.

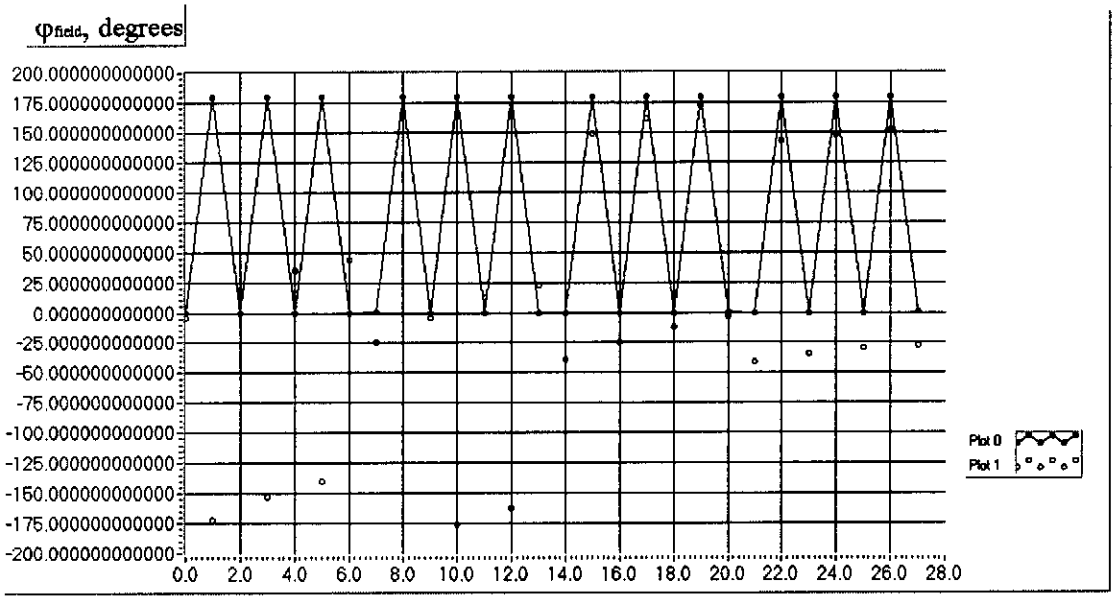

Plot 0 corresponds to free oscillation,
Plot 1 corresponds to forced oscillation at the frequency
$f_{op\ free}$=1.299999998241 Hz.

Fig.11.Phase distribution of the free and forced oscillation in the 4×7=28-cell niobium TESLA supercavity at room temperature.

One can see that relative amplitude and phase distribution of the free oscillation is very different from relative amplitude and phase distribution of the forced oscillation.

Fig.12, 13 and 14 show $|S_{11}|$, $|S_{21}|$ and φ_{21} dependence on frequency for the 4×7=28-cell niobium TESLA supercavity at room temperature. One can see that there are no $|S_{11}|_{min}$, $|S_{21}|_{max}$ and $|d\varphi_{21}/df|_{max}$ in the vicinity of an operational mode frequency. From these calculations we have obtained the following data:
frequencies corresponding to $|S_{11}|_{min}$ are equal to
1300010389 Hz (+12148 Hz) and 1300108198 Hz,
frequency corresponding to $|S_{21}|_{max}$ is equal to
1300084998 Hz (+76757 Hz),
frequencies corresponding to $|d\varphi_{21}/df|_{max}$ are equal to
1300009428 Hz (+11187 Hz) and 1300109738 Hz,
free oscillation frequency is equal to 1.299999998241 Hz.

One can see a large difference between these frequencies and a free oscillation frequency of the operational mode.

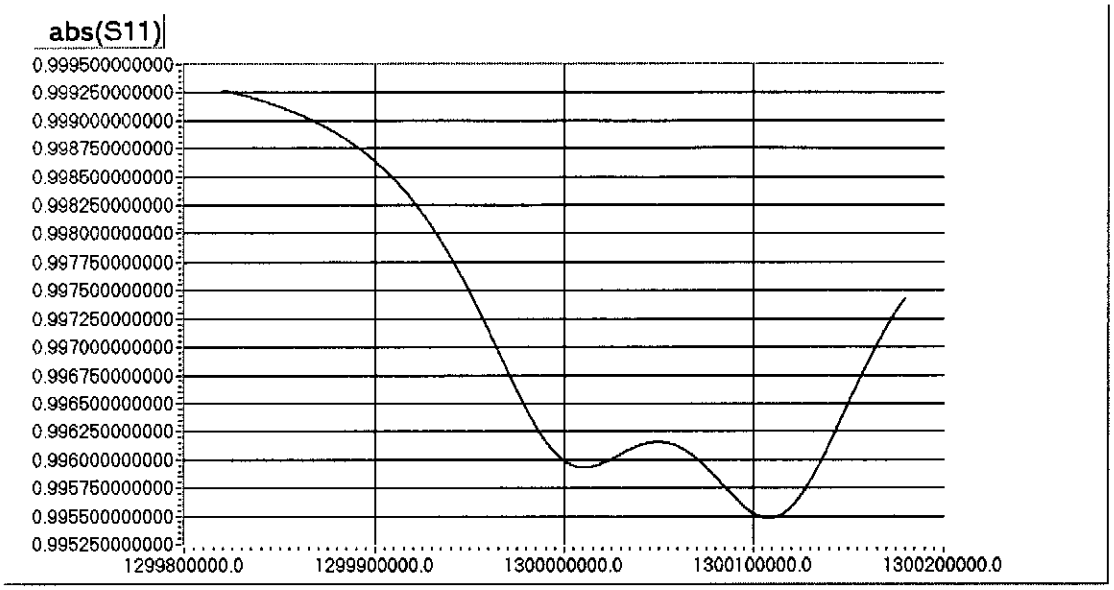

Fig.12. $|S_{11}|$ dependence on frequency for the 4×7=28-cell niobium TESLA supercavity at room temperature.

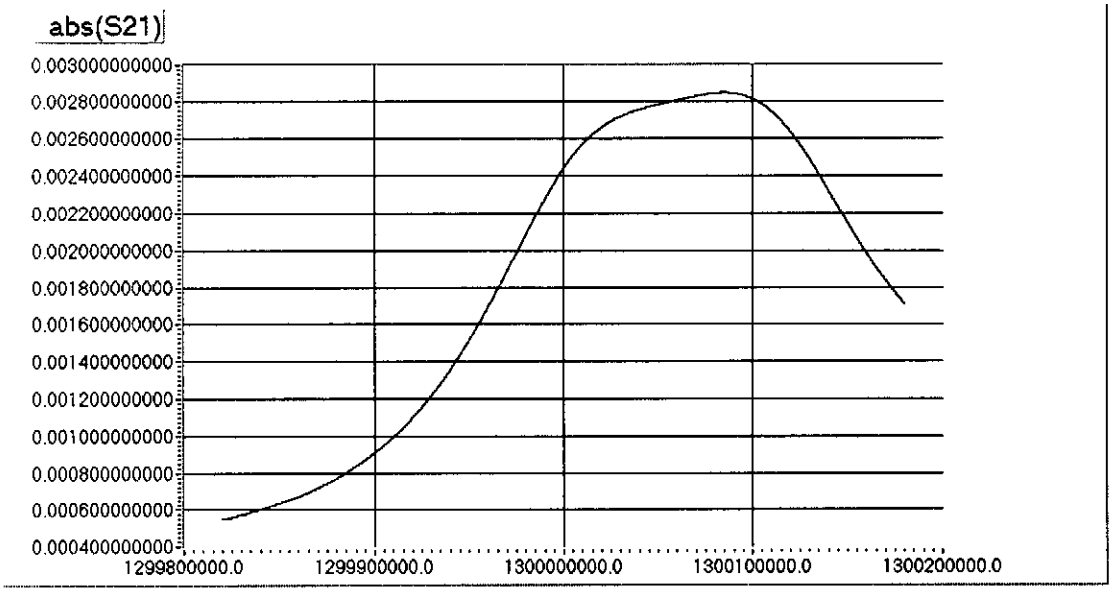

Fig.13. $|S_{21}|$ dependence on frequency for the 4×7=28-cell niobium TESLA supercavity at room temperature.

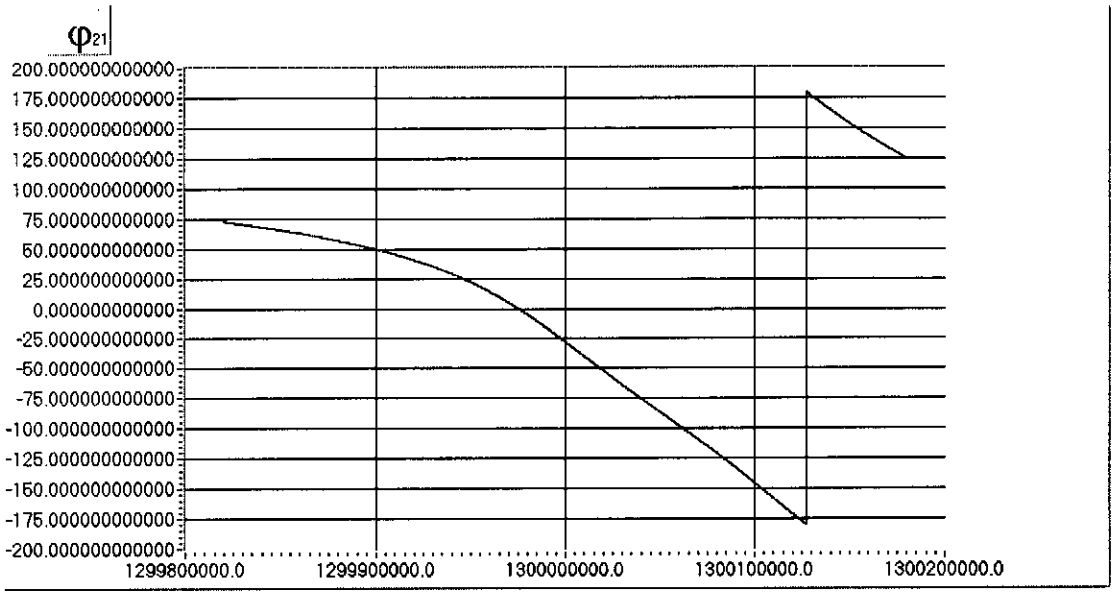

Fig.14. Transmission coefficient phase dependence on frequency for the 4×7=28-cell niobium TESLA supercavity at room temperature.

Simulation results for a different cell detuning caused by a perturbing body are shown in Table 3. These results were obtained with a direct calculation of the free oscillation frequency without and with the perturbing body in the cavity (with an ideal RPT).

Table 3.

Rel. cell detuning ($\delta f_{nb}/f_n$)	Measurement error, %	Cavity detuning Hz	Remarks
10^{-7}	0.5	5	nonrealistic case
10^{-6}	0.55	46	nonrealistic case
10^{-5}	0.95	470	nonrealistic case
5×10^{-5}	2.75	2435	acceptable value
10^{-4}	4.5	5100	acceptable value
10^{-3}	------	------	very large field perturbation
5×10^{-3}	------	------	very large field perturbation

We shall use $\delta f_{nb}/f_n=5\times10^{-5}$ in our simulation.

Fig.15 and 16 show the perturbed free oscillation field distribution when the perturbing body is inserted into the 5-th and 23-d cell.

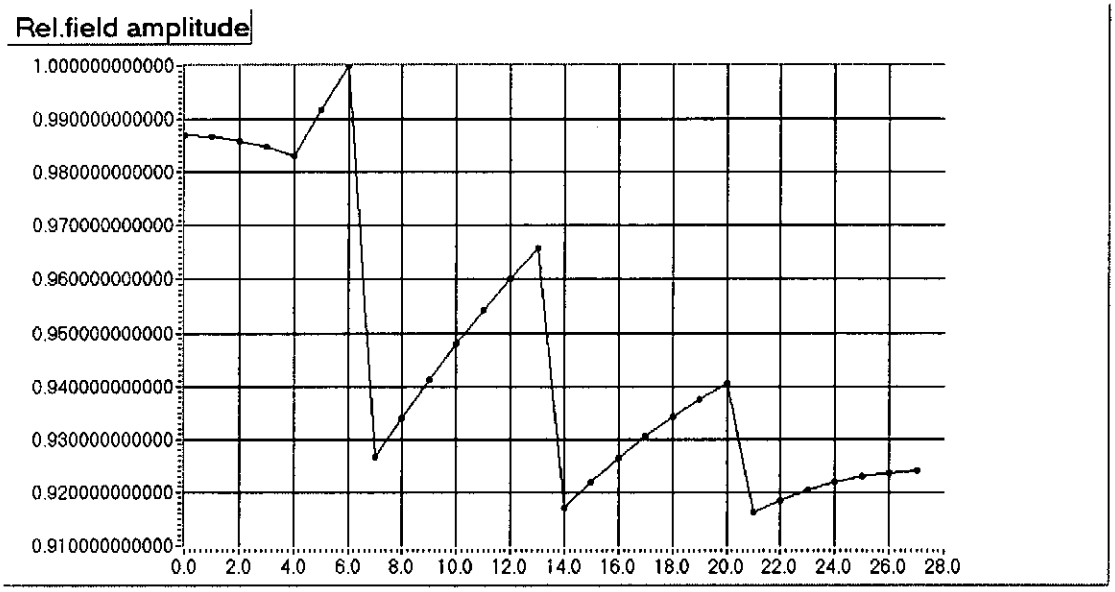

Fig.15. The perturbed free oscillation field distribution in the 4×7=28-cell niobium TESLA supercavity at room temperature. The perturbing body is inserted into the 5-th cell.

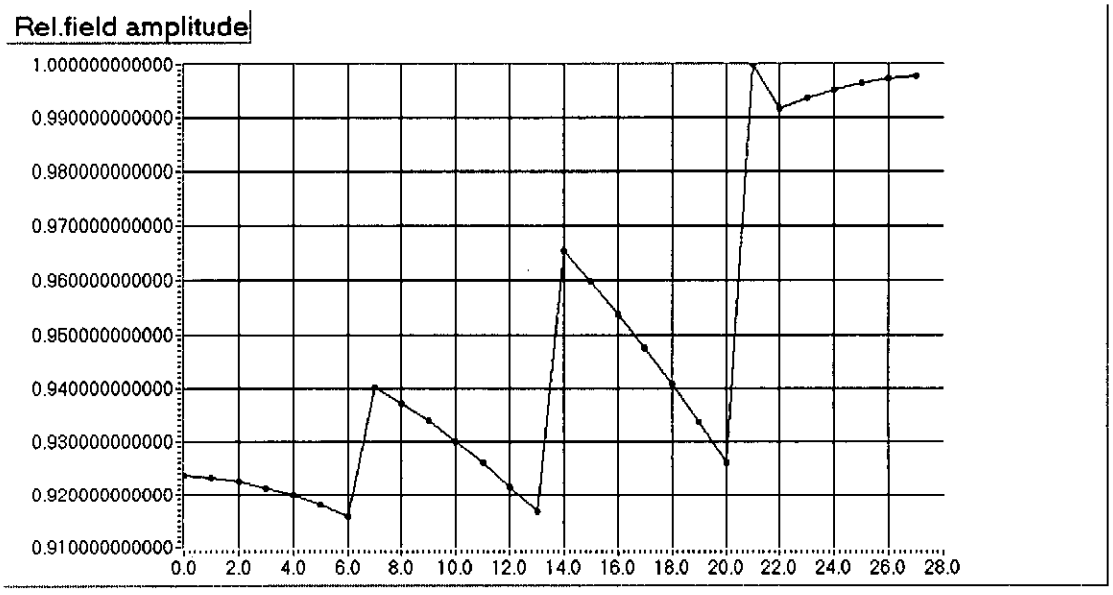

Fig.16. The perturbed free oscillation field distribution in the 4×7=28-cell niobium TESLA supercavity at room temperature. The perturbing body is inserted into the 23-d cell.

The last two figures show high sensitivity of the field distribution to the cell detuning (in our examples $\delta f_{5b}/f_5 = \delta f_{23b}/f_{23} = 5\times10^{-5}$). Fig.17 shows field measurement simulation in the 4×7=28-cell niobium TESLA supercavity at room temperature ($\delta f_{nb}/f_n=5\times10^{-5}$).

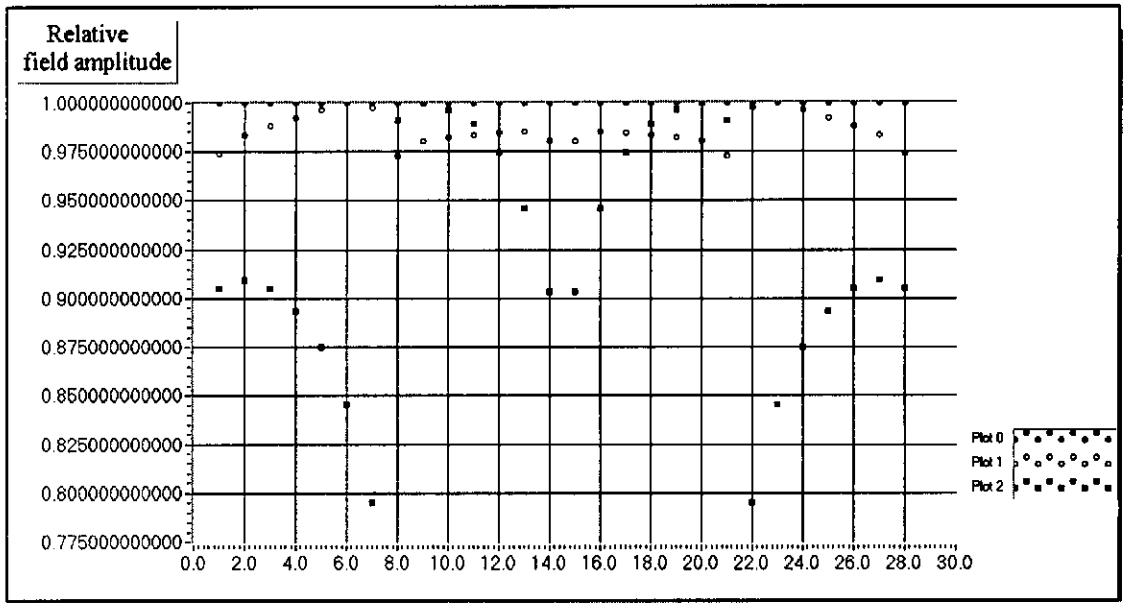

cell number, n

Plot 0 corresponds to free oscillation field distribution,
Plot 1 corresponds to an ideal RPT,
Plot 2 corresponds to f($|d\varphi_{21}/df|_{max}$)-measurement simulation.

Fig.17. Field measurement simulation in the 4×7=28-cell niobium TESLA supercavity at room temperature ($\delta f_{nb}/f_n=5\times10^{-5}$)

One can see that f ($|d\varphi_{21}/df|_{max}$)-field measurement has very large error (about 21%) and f ($|S_{21}|_{max}$)-field measurement can not be used at all.

Fig.18 shows φ_{21} dependence on cell number calculated at free oscillation frequency when a perturbing body is inserted into different cells. From this figure we can see that φ_{21} doesn't have a weak dependence on cell number as in the case of the 9-cell TESLA cavity. Fig.19 shows φ_{21}-field measurement simulation. One can see very large (20%) error in this case.

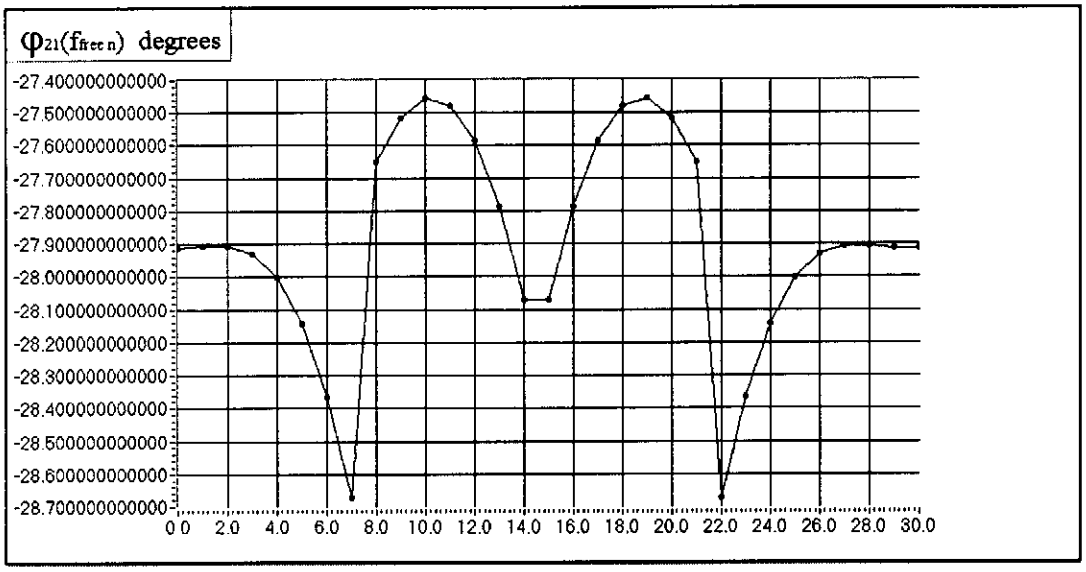

Fig.18. $\varphi_{21}(f_{free\ n})$ dependence on cell number (n=0, 29and 30 correspond to the cavity without the perturbing body)

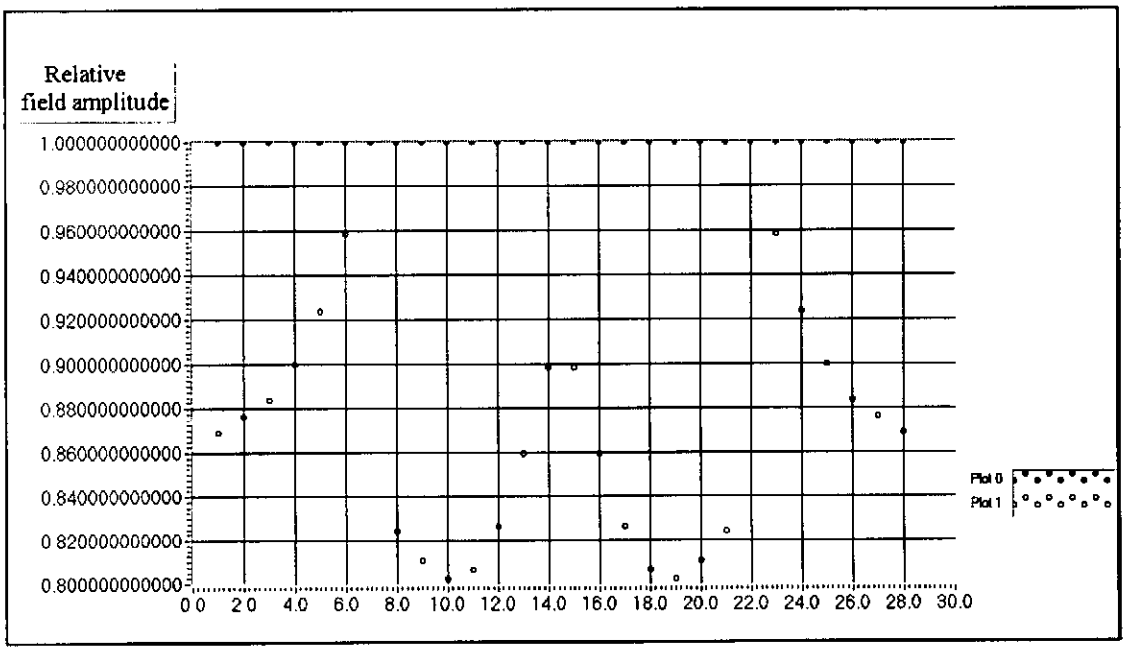

Plot 0 corresponds to free oscillation field distribution,
Plot 1 corresponds to φ_{21}-field measurement simulation.

Fig.19. φ_{21}-field measurement simulation in the 4×7=28-cell niobium TESLA supercavity at room temperature ($\delta f_{nb}/f_n=5\times10^{-5}$).

Field measurement simulation in the 4×7=28-cell copper TESLA supercavity with $Q_0=2.5\times10^4$ has shown that a measurement error is about 7% and field measurement simulation in the 51-cell cavity with an operational $\pi/2$-mode and $Q_0=10^4$ has shown 0.8% measurement error.

Fig.20 shows φ_{21}-field measurement simulation in the 51-cell cavity. Fig.20a shows a field measurement simulation result for odd cells and Fig.20b shows a field measurement simulation result for even cells. Electromagnetic field in the even cells is very weak and measurement error is very large. Field measurement error in the odd cells is only 0.8%.

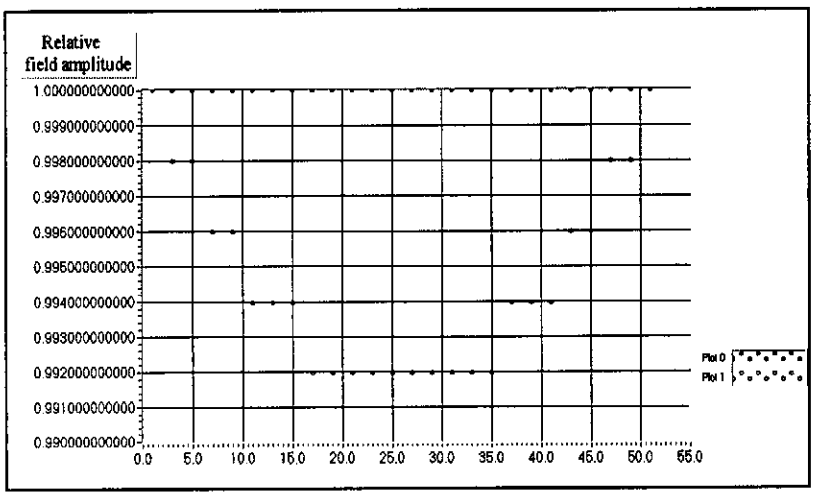

cell number, n

Fig.20a

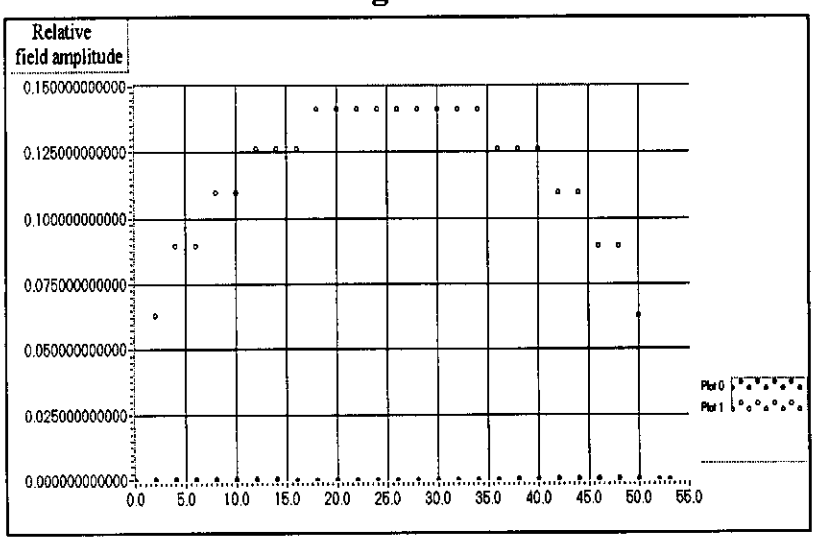

cell number, n

Fig.20b

Plot 0 corresponds to free oscillation field distribution,

Plot 1 corresponds to φ_{21}-field measurement simulation.

Fig.20. φ_{21}-field measurement simulation in the 51-cell cavity with an operational $\pi/2$-mode and $Q_0=10^4$ ($\delta f_{nb}/f_n=5\times10^{-5}$)

Field measurement simulations show that large errors in field measurement occur in the presence of the random cells detuning in the 4×7=28-cell niobium TESLA cavity at room temperature (see Fig.21).

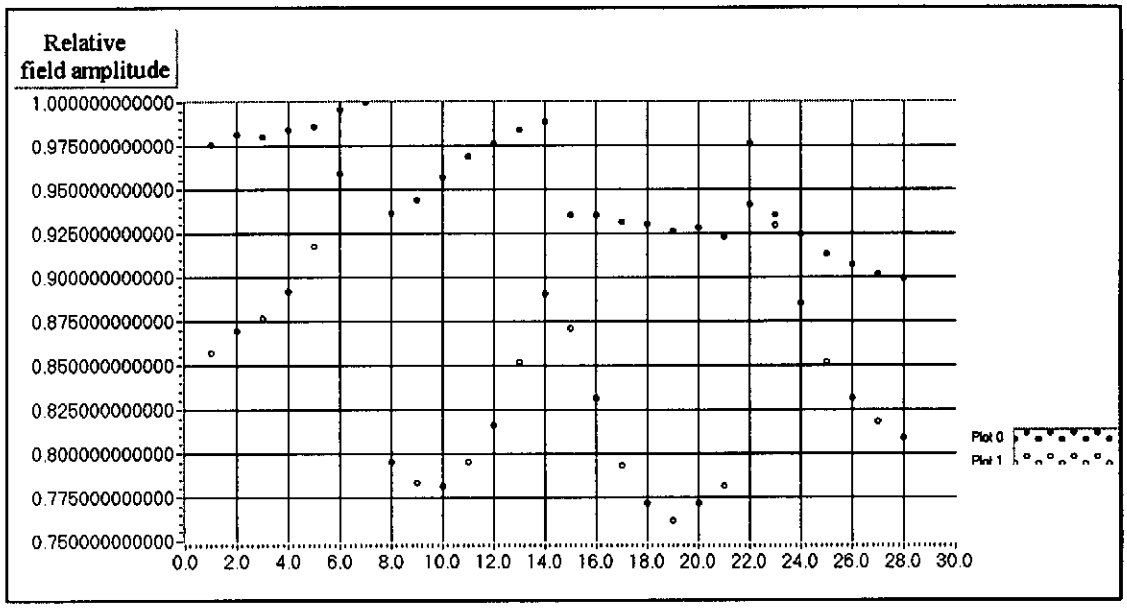

cell number, n

Plot 0 corresponds to free oscillation field distribution,
Plot 1 corresponds to φ_{21}-field measurement simulation.

Fig.21. φ_{21}-field measurement simulation in the 4×7-cell niobium supercavity at room temperature in the presence of random cells detuning ($|\delta f_{cn}|$ <50 kHz, $\delta f_{nb}/f_n=5\times10^{-5}$)

V. CONCLUTION

Field measurement accuracy in niobium TESLA cavity at room temperature was estimated. It was shown that an accuracy in the field measurement is limited by 20% in the niobium 4×7=28-cell TESLA supercavity and is less then 1% in 9-cell TESLA cavity. Large error in the 4×7=28-cell TESLA supercavity field measurement is caused by high sensitivity of the field distribution along the cavity to cells detuning and low Q_0-factor of the cells. It creates a large difference between free oscillation field distribution in the unperturbed and perturbed cavity even in the case of small ($\delta f_{nb}/f_n=5\times10^{-5}$) cell detuning caused by the perturbing body. Field measurement error less then 0.8% was obtained in the 51-cell cavity with an operational $\pi/2$-mode and low

Q_0-factor of the cells (10^4). It confirms that the main source of the field measurement error is a difference between the unperturbed and perturbed field distribution along the cavity.

Nonuniformity in the π-mode accelerating field amplitude along the cavity can be estimated with the following formula [4]

$$\sigma_{\frac{\Delta E}{E}} = 2\frac{\sigma_{\frac{\delta f_c}{f_c}}}{K_c}\sqrt{\frac{N+1}{3}\left\{N\left(1+\frac{K_c}{2}\right)^3 + (1+K_c)^3\frac{2N^2-5N+2}{5}\right\}} \approx$$

$$\approx \frac{\sigma_{\frac{\delta f_c}{f_c}}}{K_c}\sqrt{\frac{8(N+1)(N^2+1)}{15}} \qquad (4)$$

Where: $\sigma_{\Delta E/E}$ is a r.m.s. of the relative field nonuniformity,
$\sigma_{\delta f/f}$ is a r.m.s. of the relative cells detuning,
N is a number of cells in the cavity,
K_c is a coupling coefficient between cells.

The 4×7-cell supercavity has an operational 0-π-mode and its field nonuniformity cannot be estimated with formula (4). As it can be shown with a nonuniformity calculation, a 28-cell usual cavity has relative field nonuniformity about 1.3 times more then 4×7-cell cavity.

It was shown that an acceptable relative cell detuning caused by the perturbing body is equal to $(0.5 - 5)\times10^{-5}$ for 9-cell TESLA cavity and is equal to $(1 - 5)\times10^{-5}$ for the 4×7-cell TESLA supercavity.

It was shown that the best accuracy could be obtained with φ_{21}-field measurement. It should be noted that this method may give a very large errors in the cases when one of the coupling coefficients is large enough (for example $\chi_2 >> 1$ and provide travelling wave regime in the direction from the first cell to the last cell) and other coupling coefficient is very small ($\chi_1 << 1$ and provide standing wave regime when cavity is fed through the last cell). This method of field measurement gives a good result in the case when $\chi_{n1}, \chi_{n2} << 1$.

Very large difficulties can occur in measuring of the free oscillation frequency (see Fig.12, 13 and 14). These difficulties are very large in the presence of the random cells detuning.

Fig.22 shows an example of a field measurement simulation in the 4×7=28-cell superconducting TESLA cavity in the presence of a random cells detuning. One can see that 50 kHz random cells detuning creates 12% nonuniformity in the field distribution along the cavity and field measurement error achieves 3% with all measured quantities.

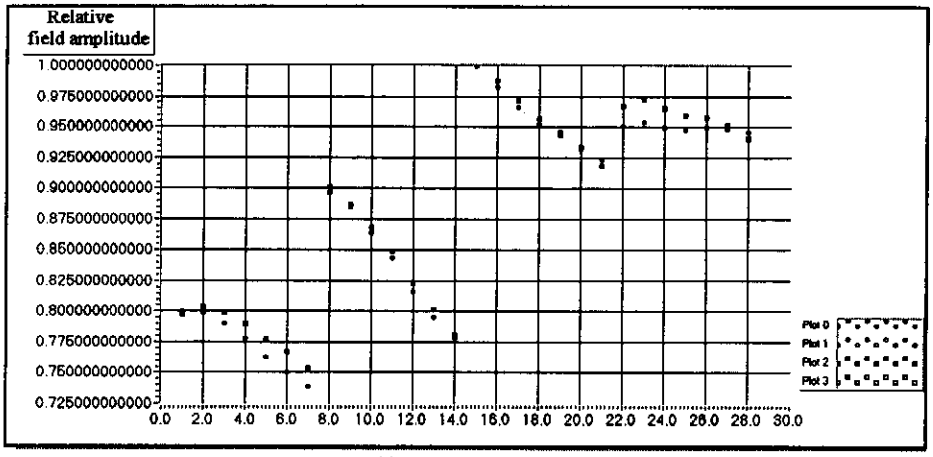

cell number, n

Plot 0 corresponds to free oscillation field distribution,
Plot 1 corresponds to an ideal RPT,
Plot 2 corresponds to f($|\, d\varphi_{21}/df\,|_{max}$)-measurement simulation,
Plot 3 corresponds to f($|\, S_{21}\,|_{max}$)-measurement simulation.

Fig.22. Field measurement simulation in the 4×7=28-cell superconducting TESLA cavity in the presence of random cells detuning
($\delta f_{nb}/f_n=5\times10^{-5}$, uniformly distributed random cells detuning is limited by ±50 kHz, $\chi_1=4.1647\times10^{4}$, $\chi_{28}=4.1647\times10^{-2}$, $Q_0=10^{10}$)

VI. REFERENCES

1. J.Sekutovich, M.Ferrario, Ch.Tang
   Superconducting Superstructure for TESLA Collider
   DESY Print, TESLA Report 96-09, August 1996.
2. Masao Nakamura
   Theory of Field Strength Determination in RF Structures
   by Perturbation Techniques
   Japanese Journal of Applied Physics, Vol.7, No.2, February 1968,
   pp.146-155.
3. M.Dohlus, N.Holtkamp, V.Kaljuzhny
   Multi-cell Cavity Excitation
   Internal Report, DESY M98-05, June 1998.
4. V.F.Vikulov , V.E.Kaljuzhny
   Effect of Errors of Fabrication on Characteristics of
   Standing Wave Accelerating Structures.
   Soviet Physics. Technical Physics, vol.50 (4), 1980, pp.460-463.
   (In English)